 doi:10.20944/preprints202007.0252.v1

Immunophenotyping of circulating leukocytes reveal non-specific activation of innate and adaptive immune systems in Multi-system Inflammatory Syndrome of Childhood Temporally Associated with SARS-Cov-2 Infection: Descriptive cohort study

Michael J. Carter[1,2 #] PhD; Matthew Fish[3,4,5 #] MSc; Aislinn Jennings[3,4,#] MSc; Katie J. Doores[4] PhD; Paul Wellman[2] BSc, Jeffrey Seow[4] PhD; Sam Acors[4] PhD; Emma Timms[5], Julia Kenny[1,2] PhD; Stuart Neil[4] PhD; Michael H. Malim[4] DPhil; Shane M. Tibby[2*] MD; Manu Shankar-Hari[3,4*] PhD

# Denote equal contributions

*Corresponding authors

Affiliations

1. Department of Women and Children's Health, King's College London, UK

2. Paediatric Intensive Care Unit, Evelina London Children's Hospital, London, UK

3. Department of Intensive Care Medicine, Guy's and St Thomas' NHS Foundation Trust, London, UK

4. Department of Infectious Diseases, School of Immunology and Microbial Sciences, King's College London

5. Peter Gorer Department of Immunobiology, School of Immunology and Microbial Sciences, King's College London

Current address, qualifications and affiliations of the Corresponding author*

Dr Manu Shankar-Hari MB BS MSc MD PhD FRCA FFICM

5th Floor, Southwark Wing, School of Immunobiology and Microbial Sciences, King's College London, London, UK, SE1 9RT

email: manu.shankar-hari@kcl.ac.uk

Main manuscript: Tables=1 and Figures=4; References = 54

Supplementary material= 24 pages; Research Check list = STROBE checklist

Key words: MIS-C, PIMS-TS, SARS-CoV-2, immunophenotyping, serology

Preprints (www.preprints.org) | NOT PEER-REVIEWED | Posted: 12 July 2020 doi:10.20944/preprints202007.0252.v1

Abstract

We describe the innate and adaptive immune system trajectory in Multi-system inflammatory syndrome of childhood (MIS-C), at *acute* (within 72 hours of hospitalization), *resolution* (at clinical improvement) and *convalescent* phase. In our cohort, in the acute phase, 68% of the children were SARS-CoV-2 seropositive, with hypercytokinenemia (high interleukin(IL)-1beta,IL-6,IL-8,IL-10,IL-17, interferon gamma), procoagulant state, myocardial dysfunction, activated neutrophils and monocytes; differential T and B cell subset lymphopenia; activated chemokine receptor type-7 positive and gamma-delta T cell subsets; antigen presenting cells had reduced HLA-DR expression; and B-cell class-switch responses occurred with illness resolution. MIS-C is an immunopathogenic illness associated with SARS-CoV-2 infections in children.

Introduction

Children, compared to adults, have been less affected in the severe acute respiratory syndrome coronavirus 2 (SARS-CoV-2) pandemic, causing coronavirus disease-19 (COVID-19). However, recent reports highlight a new clinical syndrome in children, consisting of multiorgan dysfunction, and systemic inflammation with cytokine excess[1-12], named as multisystem inflammatory syndrome in children (MIS-C) / pediatric inflammatory multisystem syndrome temporally associated with SARS-CoV-2 (PIMS-TS).

Although there are similarities between MIS-C and Kawasaki disease such as acute mucocutaneous inflammation and shock, there are major epidemiological and clinical differences. Epidemiologically, Kawasaki disease has a peak incidence around 10-months of age, is more prevalent in Asian children and in Northeast Asian countries such as Japan, with seasonal variation[13,14]. In contrast, MIS-C is reported in older children, and thus far, almost exclusively in Europe and the United States[1-12]. Clinical findings such as gastrointestinal symptoms, temporal association with the SARS-CoV-2 pandemic, leukopenia, thrombocytopenia, excess cytokines and increase in biomarkers of heart failure (such as natriuretic peptides) reported in MIS-C[1-12], are unusual in Kawasaki disease[13,14]. Therefore, MIS-C is hypothesized as a distinct immunopathogenic illness, resulting from either altered interferon responses or antibody dependent enhancement (ADE), associated with SARS-CoV-2 infections[15]. We surmised that understanding the leukocyte alterations in MIS-C would contribute towards understanding these immunopathogenic mechanisms and, would inform clinical care of this new illness.

In this context, we report a cohort study, describing the acute alterations in the circulating leukocytes in children with a diagnosis of PIMS-TS[16], which is referred to as MIS-C in this manuscript. After detailed description of clinical and laboratory characteristics similar to previous reports[1-12], we describe the immunophenotype of circulating leukocytes, at three clinically relevant illness phases: *acute* (within 72 hours of hospitalization), *resolution* (at clinical improvement defined as improved respiratory status or cardiac support and C-reactive protein (CRP) <100mg/L) and *convalescent* (at first outpatient follow-up after recovery).

Results

Patient cohort

The study cohort consisted of 25 patients, with 23 patients in T1, 14 in T2 and 10 in T3 (eFigure-1; eFigure-2). The median (IQR) age was 12.5 (7.7-14.4) years, 40% (n=10) were girls and 40% (n=10) were of white ethnicity. In our cohort, 28% (n=7) had radiological evidence of pneumonia, 56% (n=14) had vasoactive infusions, and 28% (n=7) had evidence of coronary artery aneurysm (Montreal Z-score ≥2.0[17]). Gastrointestinal symptoms were present in 72% (n=18) of the study cohort. Respiratory virus panel was negative in all patients and no bacterial infections were identified in this cohort, at hospitalization (Table-1).

Table-1. Characteristics of the study cohort

Characteristic	N = 25 patients
Age (Years, Median; IQR; Range)	12.5 (7.7–14.4; 1.1–16.8)
Female (N; %)	10 (40%)
Self-reported ethnicity	
Asian (N; %)	5 (20%)
Black (N; %)	9 (36%)
White (N; %)	10 (40%)
Other (N; %)	1 (4%)
Comorbidity* (N; %)	5 (20%)
Clinical features at presentation	
Duration of fever prior to hospitalisation (Median; IQR; Range)	5 (4–5; 0–9)
Patients meeting classical Kawasaki disease criteria (N; %)	3 (12%)
Oral mucocutaneous involvement (N; %)	6 (24%)
Bilateral non-purulent conjunctivitis (N; %)	10 (40%)
Polymorphous non-blanching rash (N; %)	12 (48%)
Erythema or oedema of hands or feet (N; %)	5 (20%)
Periungual desquamation (N; %)	0
Cervical lymphadenopathy (N; %)	4 (16%)
Respiratory distress (N; %)	4 (16%)
Tachycardia (N; %)	6 (24%)
Gastrointestinal symptoms (N; %)	18 (72%)
SOFA score at presentation (Median; IQR; Range)**	2 (1–3, 0–6)
Worst SOFA score (Median; IQR; Range)**	2 (1–5, 1–8)
Additional findings during admission	
Primary endpoint pneumonia (N; %)	7 (28%)
Worst coronary artery Z-score (Median; IQR; Range)	1.6 (0.7–2.2; -2.0–4.6)
Worst left ventricular fractional shortening (Median; IQR; Range)	27 (23–36; 15–47)

Treatments during admission	
PICU admission (N; %)	21 (84%)
Mechanical ventilation (N; %)	2 (8%)
Vasoactive infusion (N; %)	14 (56%)
High dose corticosteroids (N; %)	21 (84%)
Intravenous immunoglobulin (N; %)	23 (92%)
Biologic immunomodulation (N; %)****	15 (60%)
Outcome	
PICU length of stay (Days; Median; IQR; Range)	3 (2–5; 0–18)
Hospital length of stay (Days; Median; IQR; Range)	8 (6–10, 2–25)
Presence of coronary artery aneurysms (N; %)	7 (28%)
Myocardial infarction (N; %)	1 (4%)
Pulmonary embolus or other significant thrombus (N; %)	2 (8%)
Significant acute mental health diagnosis (N; %)	1 (4%)
SARS-Cov-2 Status	1 (4%)
SARS-Cov-2 PCR positive (N; %)	1 (4%)
SARS-Cov-2 IgG antibody positive (N; %)	17 (68%)
ID50 in seropositive patients (median (IQR); range)	474 (355 – 644; 67 - 1905)

2 children with asthma (1 with eczema and 1 with autistic spectrum disorder), 1 child with food allergy, 1 child with haemoglobin C trait, and 1 child with aplastic anaemia and immunosuppression (ciclosporin). **Variables adjusted by age group (see eTable-2 for details of SOFA score calculations). ***1 patient treated with anakinra, 4 patients with infliximab and 10 patients with tocilizumab. ** Montreal Z-score[17] ≥ 2 on echocardiography or computed tomography. Primary end-point pneumonia was defined as per Cherian T et al[18].*

SARS-CoV-2 virology, antibodies and pseudoviral neutralization assays

One patient was RT-PCR positive for SARS-CoV-2 infection. Seventeen (68%) were seropositive. Amongst the eight seronegative children, six had a clear history of either prior symptoms suggestive of SARS-CoV-2 infection, close household contact with confirmed cases of SARS-CoV-2 infection, presence at mass gatherings or parents who were health care workers. In seropositive patients, only IgG to N protein was detected, IgG for S and RBD were higher than IgM and positively correlated (Figure-1A; Figure-1B). The median (IQR) ID50 for pseudoviral neutralization assay was 474 (355 – 644) units in positive patients (eFigure-3) and positively correlated only with RBD and S IgG concentrations (Figure-1C). These findings imply that SARS-CoV-2 infections had occurred ≥2 weeks prior to clinical presentation[19,20].

Preprints (www.preprints.org) | NOT PEER-REVIEWED | Posted: 12 July 2020 doi:10.20944/preprints202007.0252.v1

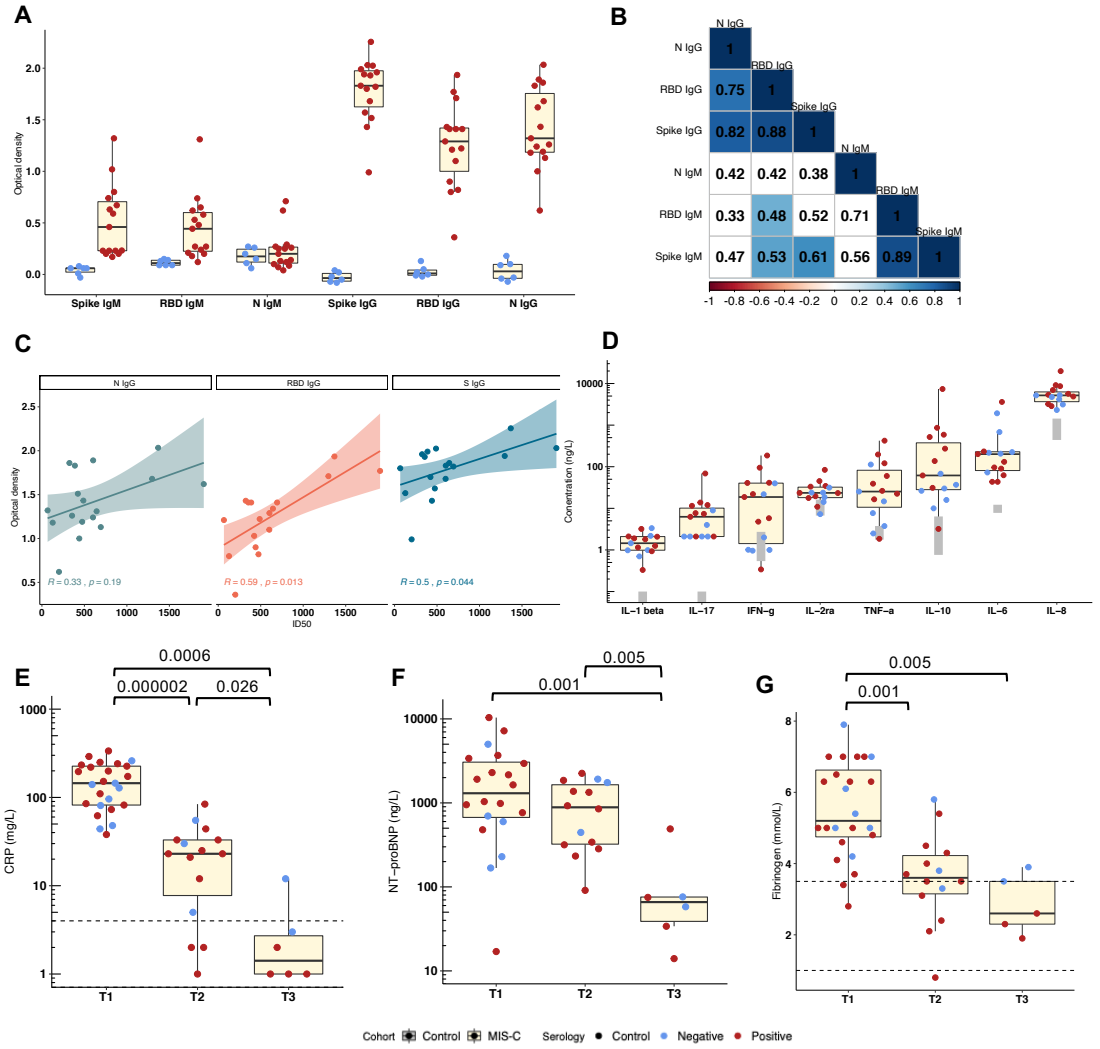

Figure- 1 SARS-CoV-2 Serology and biomarkers of inflammation, coagulation and myocardium *Serology, and cytokine profiles (n=23) were measured at T1. Clinical biomarkers were measured at acute (T1), resolution (T2) and convalescent (T3). The box and whisker plot with bottom border of the box being 25th percentile; line bisecting the shaded region of each box, median; and top border of the box, 75th percentile. For correlations spearman's rank was performed. T1 Dots are coloured by serology result; positive (red) and negative (blue). OD refers to optical density. Further details of clinical biomarkers Ferritin, Troponin, D-Dimer and platelet counts are provided in eFigure-4.* ***Figure-IA:*** *OD of IgG antibodies for N, RBD and S proteins were higher than their corresponding IgM, confirming prior SARS-CoV-2 infection;* ***Figure-IB:*** *Positive correlations were observed between IgG of N, RBD and S proteins and S IgM was also correlated to RBD IgM;* ***Figure-IC:*** *ID50 for S and RBD were positively correlated with IgG S and RBD OD;* ***Figure-ID:*** *In most patients, the cytokine levels in nanograms/Litre (IL-1beta; IL-17; IFN-G, IL-2RA, TNF-a, IL-18, IL-6, IL-8) were all log fold higher than their corresponding laboratory reference normal ranges, which are shown as grey boxes for each cytokine;* ***Figure-IE:*** *CRP levels were high in T1 and decreased over time;* ***Figure-IF:*** *Raised NT-proBNP at the acute phase suggest myocardial dysfunction, when considered with reduced left ventricular fractional shortening;* ***Figure-IG:*** *Fibrinogen levels were highest at T1 and decreased over time, implies procoagulant state in the acute phase, when considered with raised D-Dimers and low platelet counts. Abbreviations: Interleukin (IL), Interferon-Gamma (IFN-G), Tumor necrosis factor-alpha (TNF-a), IL-2 receptor alpha (IL-2RA).*

Evidence of inflammation, coagulation and myocardial dysfunction using biomarkers

In the acute phase, all the cytokines measured (IL-1beta, IL-17, IFN-G, IL-2RA, TNF-a, IL-10, IL-6, IL-8) were above the normal range (Figure-ID) alongside raised CRP and ferritin implied acute inflammation in the cohort (Figure-1E; eFigure-4A). Raised NT-Pro-BNP (Figure-1F), and impaired LV-shortening on echocardiogram (Table-1), implied myocardial dysfunction and raised troponin implies myocardial injury (eFIgure-4B). Raised fibrinogen (Figure-1G), raised D-Dimer and low platelets (eFigure-4C-D) in the acute phase, highlights a procoagulant state in these patients. These changes normalized by the convalescent phase.

Neutrophil activation and impaired antigen presentation in antigen presenting cells (APCs)

Absolute neutrophil, monocyte, DC and natural killer (NK) cell counts were similar during the acute, resolution and convalescent phases, and were similar to healthy controls (Figure-2A-D). The acute phase was characterized by raised neutrophil CD64 MFI, compared with healthy controls, implying activation, which normalized by the resolution phase (Figure-2E). The neutrophil activation inference is also supported by high levels of IL-8 in these patients. There was a concomitant decrease in CD10 MFI on neutrophils (Figure-2F). Monocyte CD14MFI, toll like receptor-4 co-receptor[21] was reduced (eFIgure-5A) and CD64 MFI was increased (eFigure-5B), implying activation and cytokine production[22,23]. Significantly decreased HLA-DR and CD86 MFI in the overall monocyte population (Figure2G-H), imply impaired antigen presentation. The classical monocyte proportions were unchanged, with a decrease in CD86MFI (eFigure-5C-D). The myeloid (conventional) DC subset decreased in the resolution phase, compared to the acute phase (Figure-2I). The DCs also had low decreased HLA-DR and CD86 MFI (Figure-2J), suggesting impaired DC function such as antigen cross presentation to CD8+ T cells and priming / polarizing of naïve helper T cells[24] (Figure-2J). There was a positive correlation between HLA-DR and CD86 MFI in monocytes and DCs (Figure2-K-L).

Preprints (www.preprints.org) | NOT PEER-REVIEWED | Posted: 12 July 2020 doi:10.20944/preprints202007.0252.v1

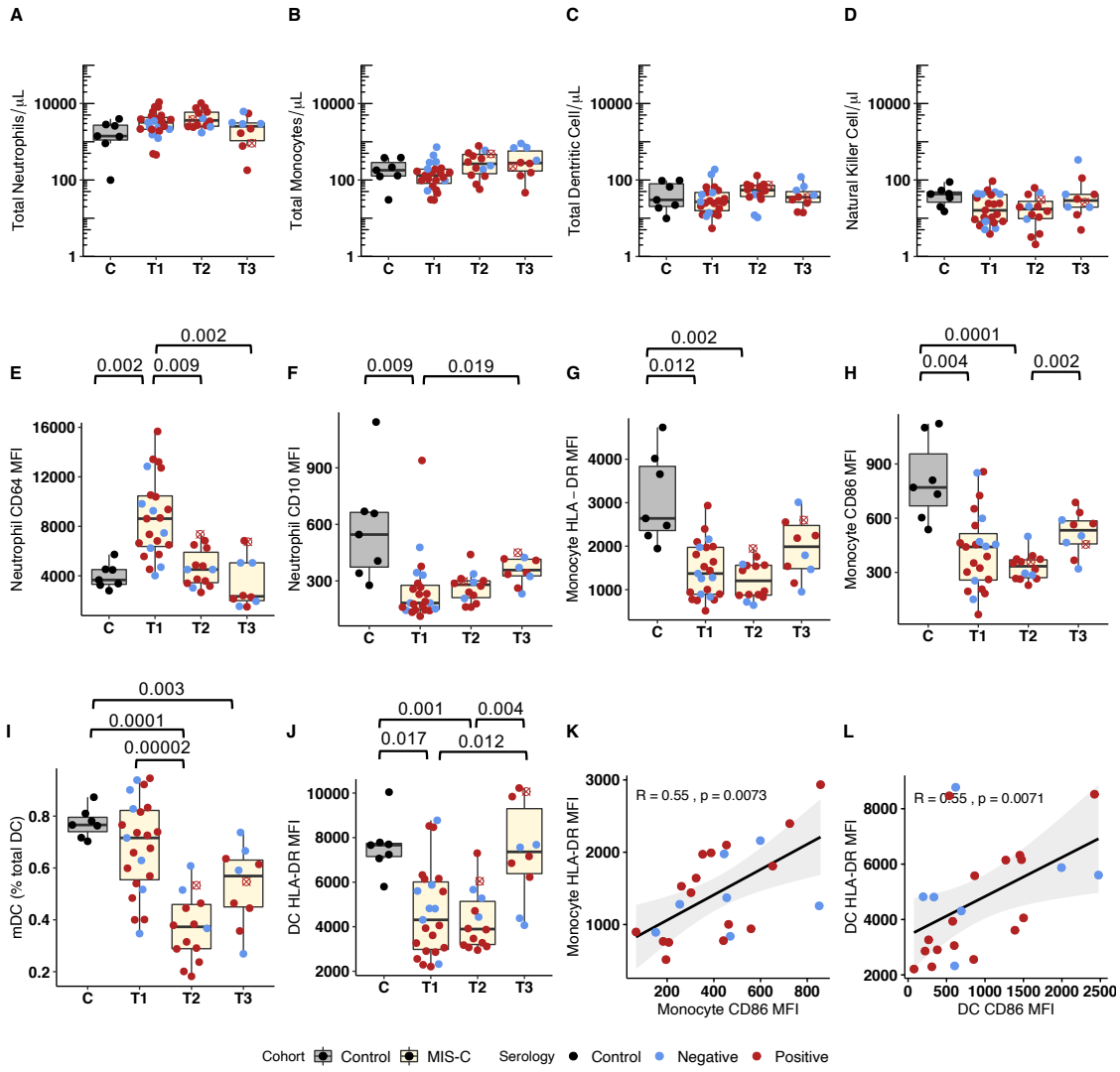

Figure-2 Innate immune cell alterations at T1, T2 and T3

Innate immune system changes were measured by flow cytometry in whole blood comparing; hospitalised controls (n =7), acute MIS-C T1 (n = 23), resolution MIS-C T2 (n= 14) and convalescence MIS-C T3 (n=10). The box and whisker plot with bottom border of the box being 25th percentile; line bisecting the shaded region of each box, median; and top border of the box, 75th percentile. For correlations spearman's rank was performed. T1 Dots are coloured by serology result; positive (red) and negative (blue). Boxplots are shaded by cohort; control (grey) and MIS-C (yellow). Further details are provided in eFigure-6. In Figures, ⊗ represents the only SARS-Co-V2 RT-PCR positive patient. ***Figure-2A:*** *The neutrophil counts were similar in MIS-C patients and controls;* ***Figure-2B:*** *The total monocyte counts were similar in MIS-C patients and controls;* ***Figure-2C:*** *The Dendritic cell counts were similar in MIS-C patients and controls;* ***Figure-2D:*** *The Natural Killer cell counts were similar in MIS-C patients and controls;* ***Figure-2E:*** *The neutrophils were activated in MIS-C patients compared to controls, as highlighted by the significantly higher CD64 MFI at T1, which decreased significantly and normalised by T2;* ***Figure-2F:*** *The neutrophils CD10 MFI, was significantly reduced at T1 in MIS-C patients compared to controls, and normalised by T3;* ***Figure-2G:*** *The monocytes HLA-DR was significantly lower in MIS-C patients compared to controls, which normalised by T3;* ***Figure-2H:*** *The monocytes CD86 was significantly lower in MIS-C patients compared to controls, which normalised by T3.* ***Figure-2I:*** *The nadir in proportions of myeloid dendritic cells (mDCs) was in T2.* ***Figure-2J:*** *The HLA-DR in DCs was significantly lower in MIS-C patients compared to controls, which normalised by T3;* ***Figure-2K:*** *There was a positive correlation between monocyte HLA-DR MFI and the co-stimulatory CD86 MFI also implies impaired antigen presentation function;* ***Figure-2L:*** *There was a*

positive correlation between DC HLA-DR MFI and the co-stimulatory CD86 MFI also implies impaired antigen presentation function.

Differential T cell depletion with evidence of activation

Pan-T cell lymphopenia observed in the acute phase, were more consistent in the seropositive patients and returned to normal by convalescence (Figure-3A-E). There were major differences in the magnitude of change in counts, in the activation status and time to normalization between T cell subsets. There were reductions in the helper (CD4+), cytotoxic (CD8+), and gamma-delta T cell counts (Figure-3B-D; eFigure-6A-E). Although CD4 HLA-DR MFI was similar to healthy controls, the CD4+CCR7+ T cells (mainly naïve T cells and a small proportion of central memory T cells) had significantly higher HLA-DR MFI, implying an activated state, during the acute phase (Figure-3F-G), in contrast to the CD4+CCR7- effector T cell subsets. The gamma-delta T cells, which have protective immunosurveillance functions[25], were significantly reduced during the acute phase, with an increase in HLA-DR MFI (Figure-3I), implying activation. By the convalescent phase, there was a significant increase in regulatory T cell counts, but the proportion of activated regulatory T cells (HLA-DR+)[26] with immunosuppressive effector functions[27], were unchanged (eFigure-6H). There were no correlations between S protein with gamma-delta T cells and with CD4+ CCR7- effector T cells (Figure-3J-K). Although, HLA-DR MFI within CD8+ T cells did not differ by CCR7 status, HLA-DR MFI on CD8+CCR7+ and CD4+CCR7+ cells were positively correlated (Figure-3L).

Preprints (www.preprints.org) | NOT PEER-REVIEWED | Posted: 12 July 2020 doi:10.20944/preprints202007.0252.v1

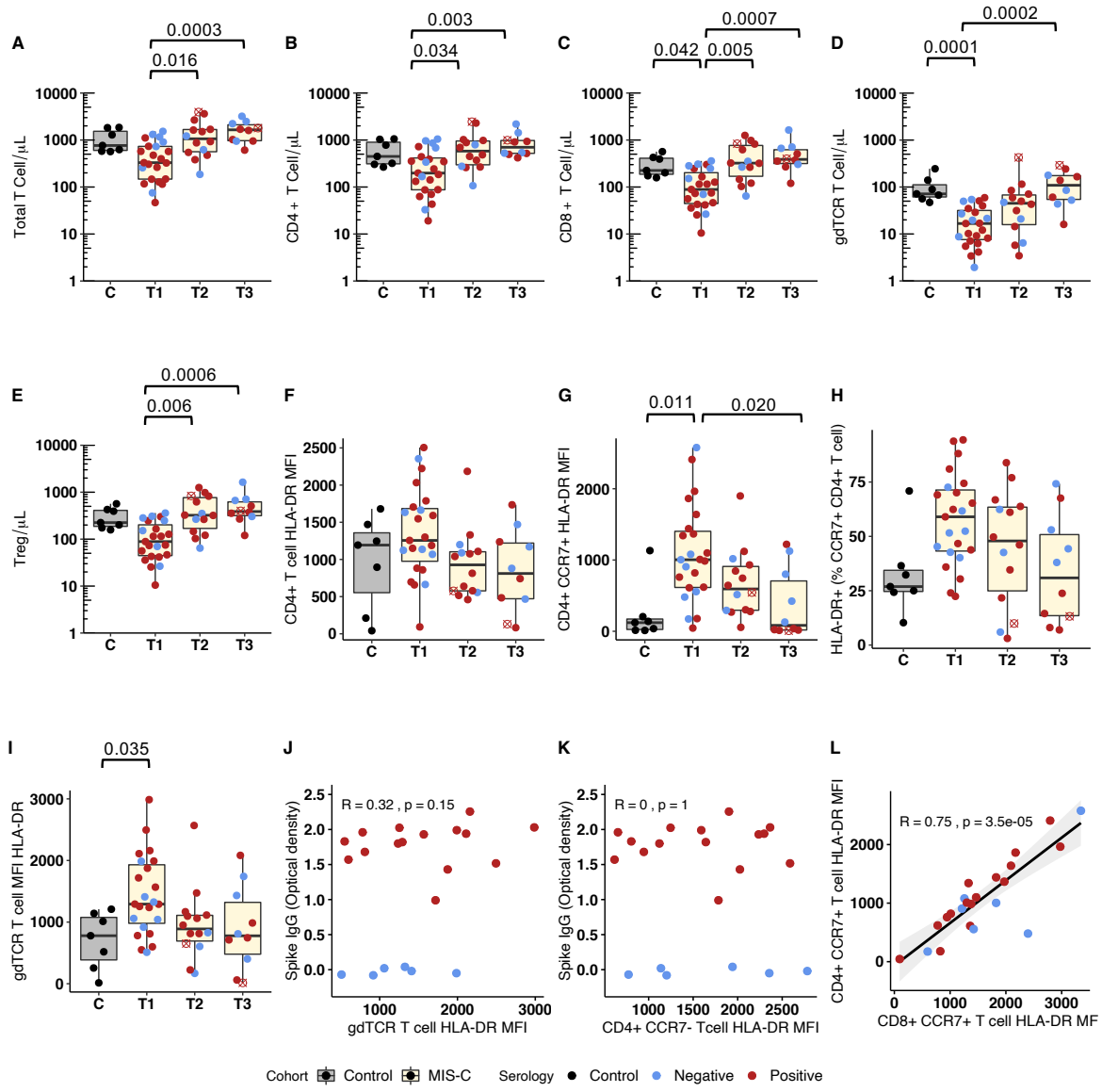

Figure-3 T cell alterations at T1, T2 and T3

T cell changes were measured by flow cytometry in whole blood comparing; hospitalised controls (n =7), acute MIS-C T1 (n = 23), resolution MIS-C T2 (n= 14) and convalescence MIS-C T3 (n=10). The box and whisker plot with bottom border of the box being 25th percentile; line bisecting the shaded region of each box, median; and top border of the box, 75th percentile. For correlations spearman's rank was performed. Dots are coloured by serology result; positive (red) and negative (blue). Boxplots are shaded by cohort; control (grey) and MIS-C (yellow). OD refers to optical density concentrations. Further details are provided in eFigure-10. In Figures, ⊗ represents the only SARS-Co-V2 RT-PCR positive patient.

Figure-3A: The absolute T lymphocyte counts were lower in MIS-C patients, compared to controls, which normalized by T2; **Figure-3B:** The total CD4+ counts were lower in MIS-C patients, compared to controls, which normalized by T2; **Figure-3C:** The CD8+ cell counts were lower in MIS-C patients, compared to controls, which normalized by T2; **Figure-3D:** The gamma-delta T cell counts had the greatest decrease of the T cell subsets in MIS-C patients, compared to controls, which normalized by T3; **Figure-3E:** The regulatory T cells were lower in MIS-C patients at acute phase, compared to controls, which increased during follow-up; **Figure-3F:** The overall CD4+ HLA-DR MFI, was similar between MIS-C patients and controls, at all-time points; **Figure-3G:** Importantly, CD4+ CCR7+ subsets had significantly higher HLA-DR MFI, implying activation, which decreased by T3; **Figure-3H:** Proportions of CD4+ CCR7+ HLA-DR positive T cell were also higher in T1 implying more activated cells; **Figure-3I:** Even though the gamma-delta T cell counts were lower in MIS-C patients, compared

to controls, these cells had high HLA-DR MFI implying activation; **Figure-3J:** There was no correlation between IgG spike protein OD values and gamma-delta T cell HLA-DR MFI; **Figure-3K:** There was no correlation between IgG spike protein and CD4+CC7+ HLA-DR MFI; **Figure-3L:** There was positive correlation between HLA-DR MFI in cytotoxic CD8+CCR7 T cells and helper CD4+CC7- T cells.

Differential B cell depletion with evidence of previous SARS-CoV-2 infection

Total B cell counts were reduced in the acute phase and the time to normalization differed between B cell subsets Figure-4A-D). The reduced natural effector cells and class switched memory B cell counts (CD19+CD27+IgM- cells) increased over time (Figure-C-D). The transitional cells were unchanged, with a progressive decrease in the proportion of B-cells with ability to produce low-affinity polyreactive antibodies (CD5+ B cell subset)[28] and an increase in the proportions of plasmablasts (CD19+CD27+++CD38+++) in some patients (Figure-2E-G). As increases in plasmablasts and class-switched memory cells were occurring in the context of profound helper T cell changes and with impaired APCs, this potentially represents a germinal center independent memory B cell response[29]. Significantly decreased HLA-DR MFI on B cells during the acute phase provide further evidence for decreased antigen presentation ability (Figure-4H). There were no correlations between S IgG and class switched memory cells and with plasmablasts (Figure-4I-J).

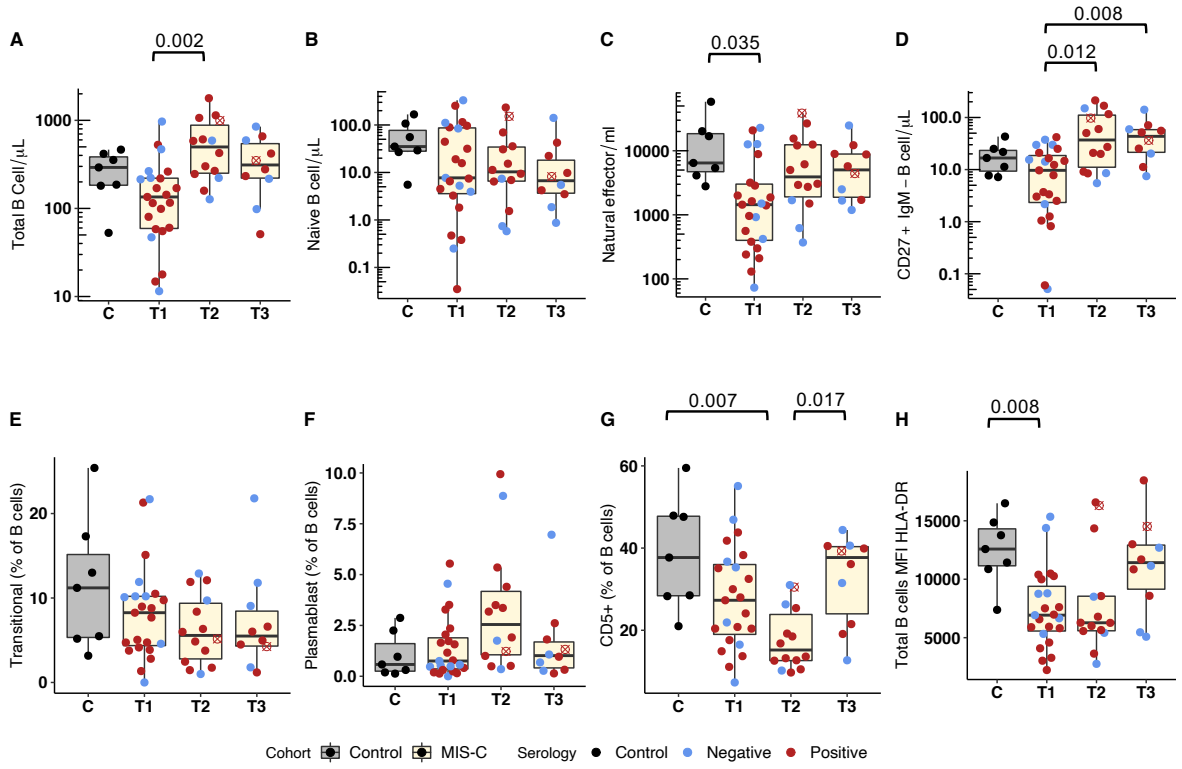

Figure-4 B cell alterations at T1, T2 and T3

B cell changes were measured by flow cytometry in whole blood comparing; hospitalised controls (n =7), acute MIS-C T1 (n = 23), resolution MIS-C T2 (n= 14) and convalescence MIS-C T3 (n=10). The box and whisker plot with bottom border of the box being 25th percentile; line bisecting the shaded region of each box, median; and top border of the box, 75th percentile. Dots are coloured by serology result; positive (red) and negative (blue). Boxplots are shaded by cohort; control (grey) and MIS-C (yellow). In Figures, ⊗ represents the only SARS-Co-V2 RT-PCR positive patient.
Figure-4A: *The absolute B lymphocyte counts were lower in most MIS-C patients, compared to controls, which normalized by T2;* ***Figure-4B:*** *The naïve B cell counts were similar between MIS-C patients and controls;* ***Figure-4C:*** *The natural effector B cell counts were lower in MIS-C patients in T1, compared to controls, which normalized by T2;* ***Figure-4D:*** *The CD27+ IgM- cell counts were similar between MIS-C patients and controls, which increased in MIS-C patients by T2, implying class switching happening at this time point in resolution of illness;* ***Figure-4E:*** *There was progressive reduction in proportion of transitional cells in MIS-C patients, compared to controls;* ***Figure-4F:*** *The proportion of plasmablasts were similar between MIS-C patients and controls, at T1 and there was an increase in proportions corresponding to increase in CD19+CD27+IgM- cells;* ***Figure-4G:*** *The CD5+ B cell changes mirrored the changes in transitional cells;* ***Figure-4H:*** *The CD19 HLA-DR MFI was lower than healthy controls in T1, which recovered to health controls MFIs by T3.*

Discussion

Our study is the first report of cellular immune changes in children with a diagnosis of MIS-C. The median age of our cohort was comparable to reported literature[4,6,8], though older than some other cohorts[1,2,5,9-11]. There were more boys in our cohort, which is consistent with larger cohort studies[6,11], but higher than other cohorts[1,2,4,8-10]. White ethnicity was more common in our cohort, which is different to other studies[2,7]. Although the proportions of seroconverted patients in our cohort (68%) was consistent with largest cohort study[11], it is lower than the reported prevalence between 80%[1,6,8] to 90%[9,10]. However, it is recognized that seroconversion may not occur in asymptomatic infections[30]. Other clinical features of our cohort were similar to the published literature[1-12], including acute inflammation, cardiac dysfunction, procoagulant state, prevalence of coronary artery aneurysms, use of intravenous immunoglobulins, use of corticosteroids and other immunomodulatory agents (***eTable-5; eTable-6***). Kawasaki Disease is characterized by neutrophilia, eosinophilia, and activation of the interleukin-1 pathways[13,14]. In contrast we observed, that the neutrophils and monocytes were activated. The APCs (monocytes, DCs, B cells) had reduced HLA-DR expression, due to raised IL-6. There was pan lymphopenia. The CD4+CCR7+ T cells and gamma-delta T cells were the only activated T cell subsets. The natural effector B cells were reduced, and the class-switch response was observed in the resolution phase. There was no discernable grouping of the immune cell changes by serological status. The major differences in the immunological changes between the different phases of illness probably represents transmuted[31] MIS-C illness trajectory, secondary to

immunomodulators administered in these patients. Studies thus far[1-12], have not performed similar follow-up assessments to make direct comparisons of this trajectory we observed. Furthermore, unlike previous studies[1-12], we report an extended cytokine profile, viral neutralization assays and in-depth description of the changes in the innate and adaptive immune cell numbers along with selected activation markers, at three clinically relevant time points.

The initiating trigger(s) and dominant immunopathogenic drivers of MIS-C illness (such as altered interferon responses and ADE[15]), are likely to differ between patients. Virus infected non-APCs recognize pathogens, triggers nuclear factor-kB (NF-kB) signaling to induce secretion of pro-inflammatory cytokines and interferon regulatory factor 3 and 7 (IRF3, IRF7) signaling mediated induction of interferon production, which helps to clear the virus and to recruit/activate further immune cells[32,33]. Altered interferon responses occur when either a high viral load at infection and/or genetic factors delay this effective early interferon mediated viral clearance[33], resulting in cytokine excess, as adaptive immune responses act to clear the virus [15,33]. Altered interferon responses may not require seropositivity and has been reported in children with severe influenzae A illness[34-36]. Altered interferon responses could be inferred in our cohort, as evidenced by raised IFN-G concentrations, and cytokine excess in presence of circulating IgG to SARS-CoV-2 antigens. In SARS and MERS coronavirus infections, ADE occurs by neutralizing antibodies mediating viral entry into Fc receptor-expressing cells[37] and IgG antibodies to S protein exacerbate lung injury in SARS infections[38]. This is in contrast to Dengue[39] and Ebola[40] infections, where sub or non-neutralizing antibodies facilitate viral entry into host cells. Two-thirds of our cohort had neutralizing antibodies, and we observed activation of Fc receptor expressing cells (high CD64 MFI in neutrophils and monocytes). Thus, although our data could support both ADE and altered interferon responses hypotheses, further studies with targeted experiments are required to confirm these mechanisms in SARS-CoV-2 infection. Larger cohort studies are also needed to explore potential genetic susceptibility[41].

This is a small, single center study, from a tertiary pediatric center, serving an ethnically diverse population. To state that MIS-C is truly distinct from Kawasaki disease, we require concurrent immunophenotyping of children with Kawasaki disease. We highlight that most MIS-C patients have evidence of SARS-CoV-2 infection, before they become acutely unwell, but did not undertake stool

virology testing to rule out viral replication occurring in the gastrointestinal tract[42]. Although an argument could be made that sensitive tests could result in misclassification of seroconversion and virology[43], none of the immune abnormalities we describe were skewed by seropositive status. We have not explored the mechanisms for the immune cell abnormalities; as, functionality of immune cells is not assessable with cells preserved in leukocyte stabilizing medium.

In conclusion, based on our cohort characteristics and the immune cell changes we observed, MIS-C is likely to be a distinct immunopathogenic illness associated with profound changes to the innate and adaptive immune cells, in children infected with SARS-CoV-2 ≥2 weeks before the onset of acute illness. Our data highlights that the value of targeted immunomodulation based on cytokine profile.

Online Methods

Please see online supplement for additional description and data

Setting and approvals

Evelina London Children's Hospital is a major tertiary referral center for pediatric infectious diseases, cardiology and intensive care, and coordinates retrieval for 2 million children in South London and Southeast England, a region which had the highest number of COVID-19 confirmed cases in the UK during the pre-recruitment and recruitment window of our cohort (***eFigure-7***). Our institution identified and reported one of the first cases series of MIS-C[2]. The current cohort study was approved by the UK Health Research Authority (20/HRA/1714)[44]. Informed consent was obtained (from parents or guardians of children < 16 years of age) by trained health professionals.

Case definitions, blood sampling and clinical data

We recruited patients to this prospective cohort study between 27th April 2020 and 25th May 2020. Children included in this cohort have not previously been reported by our group[6]. Children under the age of 18 years were potentially eligible for the study if febrile ≥ 38.0ºC. The Centre for Diseases Control definition of MIS-C, the UK Royal College of Paediatrics and Child Health definition of PIMS-TS[14], and the World health Organization definitions are shown in ***eTable-1***. We also recruited healthy children (n=7) of similar age, without any history of recent infection or immunological comorbidity, and collected blood samples as healthy controls for comparison during the study period (***eTable-2***). We collected age, sex, self-reported ethnicity, comorbidity, clinical features at presentation, organ dysfunction / support, immunomodulatory treatments given, worst sequential organ failure score (Modified SOFA score; ***eTable-3***) and the outcomes (hospital length of stay (LOS), admission to critical care (PICU), cardiac abnormalities (including left ventricular dysfunction, myocardial infarction, coronary artery dilation/aneurysms) and evidence of significant thrombi. We also collected leukocyte counts, hemoglobin, inflammation markers (C-reactive protein (CRP), ferritin), coagulation markers (D-Dimer, fibrinogen, platelets) and markers of myocardial injury / dysfunction (troponin, N-terminal pro B-type natriuretic peptide (NT-proBNP)), at the three clinically relevant illness phases described earlier: *acute* (referred as T1), *resolution* (T2) and *convalescent* (T3). Cytokine measurements (interleukin-1beta (IL-1), IL-2 receptor agonist (IL-2RA), IL-6, IL-8, IL-10, IL-17, Tumor necrosis factor-

alpha (TNF-a), and Interferon-gamma (IFN-G) were done only at T1. We ruled out other acute infections using polymerase chain reaction (PCR) to respiratory viral pathogens on nasopharyngeal or bronchoalveolar lavage (BAL), culture of blood and other relevant tissues including urine, BAL specimens and cerebrospinal fluid as indicated. Only children meeting criteria for MIS-C were included in this analysis.

SARS-CoV-2 virology, antibodies and pseudoviral neutralization assays

We assessed the SARS-CoV-2 infection status with reverse transcription real-time polymerase chain reaction of respiratory samples (RT-PCR). We quantified immunoglobulin G (IgG) and M (IgM) for Spike (S), Nucleocapsid (N), and Receptor Binding Domain (RBD) using in-house[45] enzyme-linked immunosorbent assay (ELISA) at T1 and defined a positive result as IgG to both N and S being at least 4-fold above the background. We used a SARS-CoV-2 pseudotyped virus neutralization assay, to report infectious dose-50 (ID50) measurements. Further details are provided in eMethods.

Leukocyte phenotyping

Briefly, we developed three different flow cytometry panels for standardized immunophenotyping of innate, T and B lymphocyte subsets, as per the Human Immunology Project[26]. As ADE occurs via Fc receptors[37], we considered median fluorescence intensity (MFI) of cluster of differentiation 64 (CD64), an Fc gamma receptor[46,47], as a neutrophil activation marker, and surmised that activated neutrophils could influence lymphocytes[48]. Mature neutrophils express the metalloproteinase CD10 and decrease in CD10 would enhance T cell activation[48,49]. We used Human Leukocyte Antigen-DR isotype (HLA-DR) MFI on antigen presenting cells (APCs; monocytes, dendritic cells (DCs) and B lymphocytes) and CD86 MFI on monocytes as surrogates of antigen presentation ability. HLA-DR MFI on T lymphocytes was considered as an activation marker[26].

Blood sampling consisted of 0.5millilitres of whole blood in a leukocyte stabilizing medium (Cytodelics AB, Stockholm, Sweden)[50], obtained with routine clinical samples, at the three clinically relevant illness phases described earlier: *acute* (referred as T1), *resolution* (T2) and *convalescent* (T3). Whole blood sample staining was performed as described by the manufacturer (Cytodelics AB, Stockholm, Sweden)[23]. Briefly, frozen blood samples were thawed for 1 minute in a 37^0C water bath by gently

swirling. Then, 200microlitre of blood was added to a 96-well V-bottom plate and spun at 2000 revolutions per minute (rpm) for 2 minutes. Cells were resuspended in 100microlitre of staining mix and incubated at room temperature for 20 minutes. All fluorochromes, clones and concentrations used for whole blood surface staining for flow cytometry are reported in ***eTable 4***. Flow Cytometry Standard (FCS) files acquired using BD FACSDiva™ were analysed using FlowJo[51]. Gating strategies for all panels used the Human Immunology Project[26] approach (***eFigure 8-10***). Event counts and MFIs were calculated using FlowJo for relevant markers on specific populations. Absolute cell counts were calculated using Biolegend Precision Count Beads™. Further details are provided in eMethods.

Statistical analysis

Continuous data were summarized as median and interquartile range (IQR) and categorical data presented as frequency and percentage (%). We did not perform a-priori sample size calculations. Due to limited sample size, the statistical significance reported should only be interpreted as indicative of the direction of change in biological signals. To compare differences between healthy controls and MIS-C illness phases (T1, T2 and T3), we represented data using box and whisker plots showing all the data points using *Tidyverse package*[52] and used Wilcoxon signed-rank test with Bonferroni correction for multiple comparisons. The strength and direction of association between variables was assessed using Spearman's correlation. All analyses were performed using R studio interface[53] and R[54].

References

1. Verdoni, L., *et al.* An outbreak of severe Kawasaki-like disease at the Italian epicentre of the SARS-CoV-2 epidemic: an observational cohort study. *Lancet* **395**, 1771-1778 (2020).
2. Riphagen, S., Gomez, X., Gonzalez-Martinez, C., Wilkinson, N. & Theocharis, P. Hyperinflammatory shock in children during COVID-19 pandemic. *Lancet* **395**, 1607-1608 (2020).
3. Cabrero-Hernandez, M., *et al.* Severe SARS-CoV-2 Infection in Children With Suspected Acute Abdomen: A Case Series From a Tertiary Hospital in Spain. *Pediatr. Infect. Dis. J.* **Online First**(2020).
4. Belhadjer, Z., *et al.* Acute heart failure in multisystem inflammatory syndrome in children (MIS-C) in the context of global SARS-CoV-2 pandemic. *Circulation* **0**(2020).
5. Chiotos, K., *et al.* Multisystem Inflammatory Syndrome in Children during the COVID-19 pandemic: a case series. *J Pediatric Infect Dis Soc* (2020).
6. Whittaker, E., *et al.* Clinical Characteristics of 58 Children With a Pediatric Inflammatory Multisystem Syndrome Temporally Associated With SARS-CoV-2. *JAMA* (2020).
7. Ramcharan, T., *et al.* Paediatric Inflammatory Multisystem Syndrome: Temporally Associated with SARS-CoV-2 (PIMS-TS): Cardiac Features, Management and Short-Term Outcomes at a UK Tertiary Paediatric Hospital. *Pediatr. Cardiol.*, 1-11 (2020).
8. Kaushik, S., *et al.* Multisystem Inflammatory Syndrome in Children (MIS-C) Associated with SARS-CoV-2 Infection: A Multi-institutional Study from New York City. *J. Pediatr.* (2020).
9. Capone, C.A., *et al.* Characteristics, Cardiac involvement, and Outcomes of Multisystem Inflammatory Disease of Childhood (MIS-C) Associated with SARS-CoV-2 Infection. *J. Pediatr.* (2020).
10. Toubiana, J., *et al.* Kawasaki-like multisystem inflammatory syndrome in children during the covid-19 pandemic in Paris, France: prospective observational study. *BMJ* **369**, m2094 (2020).
11. Feldstein, L.R., *et al.* Multisystem Inflammatory Syndrome in U.S. Children and Adolescents. *N. Engl. J. Med.* (2020).
12. Dufort, E.M., *et al.* Multisystem Inflammatory Syndrome in Children in New York State. *N. Engl. J. Med.* (2020).
13. Newburger, J.W., Takahashi, M. & Burns, J.C. Kawasaki Disease. *J. Am. Coll. Cardiol.* **67**, 1738-1749 (2016).
14. Rowley, A.H. & Shulman, S.T. The Epidemiology and Pathogenesis of Kawasaki Disease. *Front Pediatr* **6**, 374 (2018).
15. Rowley, A.H. Understanding SARS-CoV-2-related multisystem inflammatory syndrome in children. *Nat. Rev. Immunol.* (2020).
16. https://www.rcpch.ac.uk/resources/guidance-paediatric-multisystem-inflammatory-syndrome-temporally-associated-covid-19; Accessed on 12-June-2020
17. Dallaire, F. & Dahdah, N. New equations and a critical appraisal of coronary artery Z scores in healthy children. *J. Am. Soc. Echocardiogr.* **24**, 60-74 (2011).
18. Cherian, T., *et al.* Standardized interpretation of paediatric chest radiographs for the diagnosis of pneumonia in epidemiological studies / Thomas Cherian .... [et al.]. *Interprétation standardisée des radiographies pulmonaires pédiatriques servant au diagnostic de la pneumonie dans les études épidémiologi* (2005).
19. Sun, B., *et al.* Kinetics of SARS-CoV-2 specific IgM and IgG responses in COVID-19 patients. *Emerg Microbes Infect* **9**, 940-948 (2020).
20. Long, Q.X., *et al.* Antibody responses to SARS-CoV-2 in patients with COVID-19. *Nat. Med.* **26**, 845-848 (2020).
21. Zanoni, I. & Granucci, F. Role of CD14 in host protection against infections and in metabolism regulation. *Front Cell Infect Microbiol* **3**, 32 (2013).
22. Krutmann, J., *et al.* Cross-linking Fc receptors on monocytes triggers IL-6 production. Role in anti-CD3-induced T cell activation. *J. Immunol.* **145**, 1337-1342 (1990).
23. Tanaka, M., *et al.* Activation of Fc gamma RI on monocytes triggers differentiation into immature dendritic cells that induce autoreactive T cell responses. *J. Immunol.* **183**, 2349-2355 (2009).
24. Freer, G. & Matteucci, D. Influence of dendritic cells on viral pathogenicity. *PLoS Pathog.* **5**, e1000384 (2009).
25. Vantourout, P. & Hayday, A. Six-of-the-best: unique contributions of gammadelta T cells to immunology. *Nat. Rev. Immunol.* **13**, 88-100 (2013).
26. Maecker, H.T., McCoy, J.P. & Nussenblatt, R. Standardizing immunophenotyping for the Human Immunology Project. *Nat. Rev. Immunol.* **12**, 191-200 (2012).

27. Vignali, D.A., Collison, L.W. & Workman, C.J. How regulatory T cells work. *Nat. Rev. Immunol.* **8**, 523-532 (2008).
28. Dono, M., Cerruti, G. & Zupo, S. The CD5+ B-cell. *Int. J. Biochem. Cell Biol.* **36**, 2105-2111 (2004).
29. Akkaya, M., Kwak, K. & Pierce, S.K. B cell memory: building two walls of protection against pathogens. *Nat. Rev. Immunol.* **20**, 229-238 (2020).
30. Long, Q.X.*, et al.* Clinical and immunological assessment of asymptomatic SARS-CoV-2 infections. *Nat. Med.* (2020).
31. Feudtner, C. A disease in motion: diabetes history and the new paradigm of transmuted disease. *Perspect. Biol. Med.* **39**, 158-170 (1996).
32. Iwasaki, A. & Medzhitov, R. Regulation of adaptive immunity by the innate immune system. *Science* **327**, 291-295 (2010).
33. Park, A. & Iwasaki, A. Type I and Type III Interferons - Induction, Signaling, Evasion, and Application to Combat COVID-19. *Cell Host Microbe* **27**, 870-878 (2020).
34. Hall, M.W.*, et al.* Innate immune function and mortality in critically ill children with influenza: a multicenter study. *Crit. Care Med.* **41**, 224-236 (2013).
35. Coates, B.M., Staricha, K.L., Wiese, K.M. & Ridge, K.M. Influenza A Virus Infection, Innate Immunity, and Childhood. *JAMA Pediatr* **169**, 956-963 (2015).
36. Oshansky, C.M.*, et al.* Mucosal immune responses predict clinical outcomes during influenza infection independently of age and viral load. *Am. J. Respir. Crit. Care Med.* **189**, 449-462 (2014).
37. Wan, Y.*, et al.* Molecular Mechanism for Antibody-Dependent Enhancement of Coronavirus Entry. *J. Virol.* **94**(2020).
38. Liu, L.*, et al.* Anti-spike IgG causes severe acute lung injury by skewing macrophage responses during acute SARS-CoV infection. *JCI insight* **4**(2019).
39. Katzelnick, L.C.*, et al.* Antibody-dependent enhancement of severe dengue disease in humans. *Science* **358**, 929-932 (2017).
40. Takada, A., Feldmann, H., Ksiazek, T.G. & Kawaoka, Y. Antibody-dependent enhancement of Ebola virus infection. *J. Virol.* **77**, 7539-7544 (2003).
41. Ellinghaus, D.*, et al.* Genomewide Association Study of Severe Covid-19 with Respiratory Failure. *N. Engl. J. Med.* (2020).
42. Lamers, M.M.*, et al.* SARS-CoV-2 productively infects human gut enterocytes. *Science*, eabc1669 (2020).
43. Krammer, F. & Simon, V. Serology assays to manage COVID-19. *Science* **368**, 1060-1061 (2020).
44. https://www.diamonds2020.eu/about/ ; Accessed on June-18-2020
45. Pickering, S.*, et al.* Comparative assessment of multiple COVID-19 serological technologies supports continued evaluation of point-of-care lateral flow assays in hospital and community healthcare settings. *medRxiv*, 2020.2006.2002.20120345 (2020).
46. Wang, Y. & Jonsson, F. Expression, Role, and Regulation of Neutrophil Fcgamma Receptors. *Front. Immunol.* **10**, 1958 (2019).
47. Pincetic, A.*, et al.* Type I and type II Fc receptors regulate innate and adaptive immunity. *Nat. Immunol.* **15**, 707-716 (2014).
48. Costa, S., Bevilacqua, D., Cassatella, M.A. & Scapini, P. Recent advances on the crosstalk between neutrophils and B or T lymphocytes. *Immunology* **156**, 23-32 (2019).
49. Marini, O.*, et al.* Mature CD10(+) and immature CD10(-) neutrophils present in G-CSF-treated donors display opposite effects on T cells. *Blood* **129**, 1343-1356 (2017).
50. http://www.cytodelics.com/uploads/1/2/3/5/123585057/whole_blood_processing_kit_protocol_ver106.pdf ; Accessed on 18-June-2020
51. FlowJo™ Software (when applicable add—for Windows or for Mac) [software application] Version 10.6.2. Ashland, OR: Becton, Dickinson and Company; 2019
52. Wickham, H.*, et al.* Welcome to the Tidyverse. *Journal of Open Source Software* **4**(2019).
53. RStudio Team (2020). RStudio: Integrated Development for R. RStudio, PBC, Boston, MA URL http://www.rstudio.com/.
54. R Core Team (2020). R: A language and environment for statistical computing. R Foundation for Statistical Computing, Vienna, Austria. URL http://www.R-project.org/.

Article Information

Author affiliations

Drs Carter, Wellman, Kenny, Fish, Jennings, Tibby, and Shankar-Hari had full access to all the data in the study and take responsibility for integrity of data. Dr Doores, Dr Acord and Dr Seow performed the ELISA and viral neutralization assays. Mr Fish, Ms Jennings, Dr Timms performed all the flowcytometry optimization and analyses.
Drs Carter, Fish, and Shankar-Hari takes responsibility for the accuracy of the data analyses.
Concept and design: Carter, Shankar-Hari
Statistical analysis: Carter, Fish, and Shankar-Hari
Drafting of manuscript: Carter, Fish, Jennings, Shankar-Hari
Acquisition, analysis and interpretation of data: All authors
Critical revision of the manuscript for important intellectual content: All authors
Obtained funding: Carter, Tibby, Shankar-Hari
Administrative, technical, or material support: Tibby, Shankar-Hari
Supervision: Shankar-Hari

The authors' COI: The authors declare no conflict of interest.

Funding/Support

The study was supported by the King's Together COVID-19 seed funds (MJC, MSH, KD, SN, MHM). MJC is supported by a National Institute of Health Research Academic Clinical Lectureship. MF is supported by National Institute of Academic Anesthesia BJA-RCOA fellowship (WKRO-2018-0047). AJ is supported by Critical Care Department at Guy's and St Thomas' Hospital PhD Funds. SA was supported by an MRC-KCL Doctoral Training Partnership in Biomedical Sciences industrial Collaborative Award in Science & Engineering (iCASE) in partnership with Orchard Therapeutics (MR/R015643/1). MSH is supported by the National Institute for Health Research Clinician Scientist Award (CS-2016-16-011). The views expressed in this publication are those of the author(s) and not necessarily those of the NHS, the National Institute for Health Research or the Department of Health and Social Care. This research was funded/supported by the National Institute for Health Research (NIHR) Biomedical Research Centre based at Guy's and St Thomas' NHS Foundation Trust and King's College London and/or the NIHR Clinical Research Facility. The views expressed are those of the authors and not necessarily those of the NHS, the NIHR or the Department of Health.

Role of funding source

The funding source did not have any role in the design, conduct or interpretation of study results.

Data sharing

Data will be available on request from corresponding authors.

Acknowledgements

We thank the parents and children who agreed to take part in this work. We thank Jennifer Irons and the Evelina Diamonds Study team and Evelina PIMS-TS Working Group. We thank the flow cytometry core at the KCL NIHR Biomedical Research Centre and for logistical support we thank Professor Matt Brown, Richard Ellis, Shaun Cochrane, Celine Trouillet. Thank you to Florian Krammer (Icahn School of Medicine at Mount Sinai) for provision of the RBD expression plasmid, Philip Brouwer, Marit van Gils and Rogier Sanders (The University of Amsterdam) for the S expression plasmid and Leo James, Jakub Luptak and Leo Kiss (LMB, Cambridge) for the provision of purified N protein. Development of SARS-CoV-2 reagents (RBD) was partially supported by the NIAID Centers of Excellence for Influenza Research and Surveillance (CEIRS) contract HHSN272201400008C.